Received: 19 September 2023 | Revised: 17 November 2023 | Accepted: 20 November 2023 | Published online: 23 November 2023

RESEARCH ARTICLE

Journal of Optics and Photonics Research
2024, Vol. 1(1) 43–49
DOI: 10.47852/bonviewJOPR32021750

BON VIEW PUBLISHING

# Tailored Dispersion and Nonlinear Effects in Flint Glass Honeycomb PCF for Optical Communication

**Amit Halder[1,2,*], Md. Riyad Tanshen[2], Mir Afzal Hossain[3], Mst. Shanjida Akter[2] and Md. Ashik Sikdar[2]**

[1]*Department of Electrical and Electronic Engineering, Rajshahi University of Engineering and Technology, Bangladesh*

[2]*Department of Electrical and Electronic Engineering, World University of Bangladesh, Bangladesh*

[3]*Department of Electrical Engineering, Arizona State University, USA*

**Abstract:** This paper describes a highly nonlinear flint glass-based honeycomb photonic crystal fiber (FGH-PCF) with a wavelength of 1550 nm. The PCF's distinctive honeycomb lattice structure, combined with the nonlinear capabilities of flint glass, enables a wide range of nonlinear optical applications. To adjust the PCF's dispersion and nonlinear effects, numerical simulations and optimization approaches were used. To achieve maximum performance, fabrication procedures were carefully regulated. Dispersion values of −436.6 ps/(nm.km) for x polarization and −448.1 ps/(nm.km) for y polarization were verified by experimental characterization. The PCF displayed low confinement losses of 2.289 dB/cm (x polarization) and 4.935 dB/cm (y polarization), as well as birefringence of $2.202\times10^{-3}$. The PCF measured 558.8 and 547.9 $W^{-1}$ $km^{-1}$ for x and y polarization, respectively, indicating a high nonlinear coefficient. The highly nonlinear FGH-PCF shows promising potential for nonlinear optical applications such as four-wave mixing, supercontinuum generation, frequency conversion, and parametric amplification. This research paves the way for compact and efficient nonlinear devices in modern optical communication systems and other cutting-edge technologies.

**Keywords:** flint glass-based honeycomb photonic crystal fiber (FGH-PCF), nonlinear optics, dispersion compensation, honeycomb lattice structure, supercontinuum generation

## 1. Introduction

Recent years have seen a lot of interest in photonic crystal fibers (PCFs) because of their distinctive optical properties and diverse range of applications (Bjarklev et al., 2003). The ability to customize these fibers' dispersion and nonlinear effects has created new opportunities for nonlinear optical devices and systems (Dudley & Taylor, 2009). Nonlinear optics has made significant development, owing to the desire for quicker, more efficient, and smaller optical communication systems, as well as cutting-edge technology (Weiner, 2011). Nonlinear optical phenomena, such as four-wave mixing, supercontinuum generation, frequency conversion, and parametric amplification, offer valuable tools for signal processing, wavelength conversion, and optical amplification (Webb et al., 2014). Realizing the full potential of these nonlinear effects often relies on the properties of the optical fibers employed. Conventional optical fibers based on silica have limitations when it comes to nonlinear applications (Cavillon et al., 2018). Therefore, researchers have been exploring alternative materials and fiber structures to enhance nonlinear effects and enable new functionalities. Among these materials, flint glass stands out for its excellent nonlinear properties, making it a promising candidate for high-performance photonic devices (Schodek et al., 2009). Honeycomb lattice structures in PCFs have gained attention due to their unique geometrical arrangement and the resulting optical properties (Broeng et al., 1999). By confining light within air or glass-filled holes arranged in a honeycomb lattice, these fibers offer precise control over the dispersion and modal properties. This enables researchers to achieve high levels of nonlinearity and birefringence, both essential factors for various nonlinear optical applications (Papadopoulos et al., 2006). Hasan et al. (2016) used a silica-based anti-resonant hollow-core fiber filled with supercritical xenon to achieve high nonlinearity of 6.74 $\times 10^{-3}$ $W^{-1}$ $km^{-1}$ in the mid-IR spectral band. Islam et al. (2017) demonstrated a PCF design with tunable dispersion characteristics by introducing an artificial flaw along one of the regular square axes. Under the working wavelength, the suggested PCF exhibited strictly single-mode behavior, with an ultra-high negative dispersion range from -584.60 to -2337.60 ps/(nm•km) and a high nonlinearity order of 131.91 $W^{-1}$ $km^{-1}$ (Islam et al., 2017). Prajapati et al. (2019) suggested an octagonal PCF design with redesigned cladding air holes, exhibiting strong birefringence, high negative dispersion (−722.48 ps/(nm•km)), and low confinement loss (0.117 dB/km) at 1.55 μm. The fiber also has a nonlinear coefficient of 21.23 $W^{-1}$ $km^{-1}$ at 1550 nm (Prajapati et al., 2019). Halder and Anower (2019) reported the development

*Corresponding author: Amit Halder, Department of Electrical and Electronic Engineering, Rajshahi University of Engineering and Technology and Department of Electrical and Electronic Engineering, World University of Bangladesh, Bangladesh. Email: amit.rueten@gmail.com

of a highly birefringent hybrid PCF (Hy-PCF) with an optimal design for broadband compensation in the S, C, and L communication bands (1400–1625 nm). They acquired exceptional features through simulations, including a high birefringence of $3.039 \times 10^{-2}$ and a high nonlinear coefficient of 33.76 $W^{-1}$ $km^{-1}$ at an effective wavelength of 1550 nm. The fiber also showed outstanding dispersion compensation capabilities across all communication bands, with a negative dispersion coefficient of -378.6 ps/(nm.km) at 1550 nm and a relative dispersion slope similar to that of a single-mode fiber (Halder & Anower, 2019). Halder (2020) presented an optimized hybrid dispersion compensating fiber with high birefringence that covers the S, C, and L communication bands. The fiber has a negative dispersion of −606 ps/(nm•km) at 1550 nm, a relatively higher birefringence of $3.76\times 10^{-2}$, low confinement loss, and a highly nonlinear coefficient of 50.34 $W^{-1}$ $km^{-1}$, making it suitable for high-rate communication systems and potentially applicable in sensing applications (Halder, 2020). A modified square-shaped PCF with extraordinary qualities was first reported by Paul et al. (2022). These features include a very high negative dispersion coefficient of −2357.54 ps/(nm.km) at 1550 nm wavelength and a substantial nonlinear coefficient of 74.68 $W^{-1}$ $km^{-1}$. To obtain outstanding results, Singh et al. (2022) investigated a unique PCF with four air-filled holes in the core and four square air holes organized in a circular pattern in the cladding. The PCF is promising for a variety of applications, including residual dispersion compensation, supercontinuum generation, and high bit rate transmission, without the need for nonlinear materials or liquids (Singh et al., 2022). They demonstrated impressive properties, including a record-high nonlinear coefficient of 85 $W^{-1}$ $km^{-1}$ at 1.55 **µ**m and a substantial negative dispersion of −597 ps/(nm.km) at the same wavelength.

In this study, a highly nonlinear flint glass-based honeycomb PCF (FGH-PCF) is presented, which has been carefully designed and optimized for operation at a specific wavelength of 1550 nm. The ultra-high nonlinear coefficient (558.8 $W^{-1}$ $km^{-1}$for × polarization) of the fiber, attributed to its geometry and the use of flint glass material, makes it well-suited for applications requiring efficient nonlinear interactions. To ensure accurate performance, numerical techniques were employed to carefully simulate and optimize the dispersion and nonlinear effects of the fiber. The simulation characterization of the fiber confirmed exceptional dispersion values, birefringence, and low confinement losses for both x and y polarizations. Tremendous promise is held by the high nonlinear coefficient and unique lattice structure of the presented PCF for various nonlinear optical applications. These applications range from advanced signal processing and frequency conversion to supercontinuum generation and parametric amplification.

## 2. Design Techniques

Figure 1 depicts a cross-sectional image of the honeycomb lattice structure suggested for the FGH-PCF. The fiber is made up of an eight-layered honeycomb lattice with a pitch (unit lattice distance). The ratio of the hole diameter (d) to the pitch (Λ), denoted as d/Λ, determines the filling fraction or air-filling fraction (AFF). To optimize the fiber's performance, specific parameter values are set, including $d_1 = 0.72$ **µ**m, $d_2 = d_3 = d_4 = d_5 = d_6 = d_7 = d_8 = d = 0.81$ **µ**m, and $\Lambda = 0.9$ **µ**m. Flint glass is chosen as the background material due to its excellent optical transmittance, and the traditional lead (II) oxide content has been replaced with other metal oxides like titanium dioxide and zirconium dioxide to address pollution concerns without

**Figure 1**
**The proposed flint glass-based honeycomb lattice PCF (FGH-PCF) in cross section. In this case, $\Lambda = 0.9$ µm, $d_1/\Lambda = 0.8$, and $d/\Lambda = 0.9$**

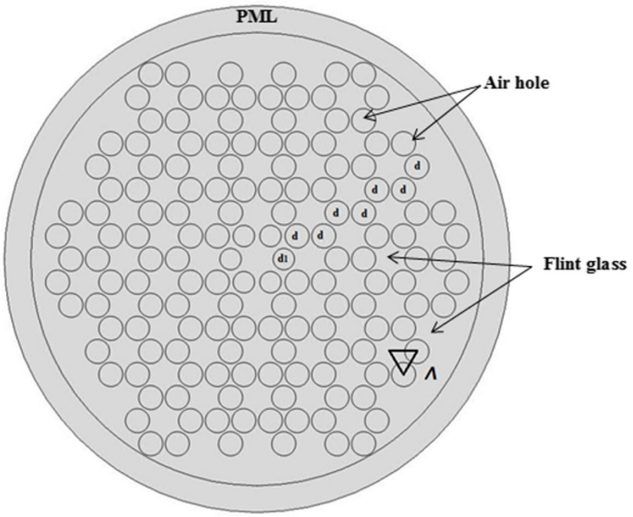


significantly affecting the glass's optical characteristics (Brain, 2002). The production process is aided by the design's simplicity, modest AFF, and circular air cavities, with commercial fiber fabrication processes like stack and draw (Pysz et al., 2014), die-cast (Zhou et al., 2006), drilling (Zhang et al., 2015), and sol-gel (Wang et al., 2013). The development of the highly nonlinear FGH-PCF involved a precise fabrication process utilizing the commercially available sol-gel technique. This method was selected for its efficiency in minimizing material wastage and enabling precise design adjustments. The optimization of the FGH-PCF's dispersion values and nonlinear coefficient was achieved through extensive numerical simulations using the finite element method (FEM). Various parameters such as pitch ($\Lambda$), hole diameter ($d$), and specific compositions of the flint glass material were systematically varied in multiple simulation iterations. Different pitch values were explored to reduce dispersion and enhance the nonlinear coefficient. The optimal pitch value, balancing superior performance and practical fabrication feasibility, was carefully determined in this study. The pitch value was set at 0.9 **µ**m for this study, with other air hole diameters being dependent on this value due to the air-filled fraction ratio (d/Λ) determining the diameter. The sol-gel technique, a widely adopted method in material science, was employed to fabricate PCFs due to its exceptional precision and versatility. By utilizing this technique, intricate nanostructured materials for PCFs can be meticulously synthesized, offering superior control over the fiber's properties. The sol-gel process allows for the seamless integration of various materials, enabling the design and production of PCFs with tailored characteristics, making it a fundamental approach in advancing the field of photonic technologies (El Hamzaoui et al., 2020).

## 3. Simulation Methodology

The optical properties of the proposed FGH-PCF are determined using the FEM (Jagota et al., 2013). The simulation tool used for this purpose is COMSOL Multiphysics version 4.2,

which provides guiding characteristics for wavelengths ranging from 1.28 μm to 1.79 μm, including the E to L wave bands (Karamifard, 2022). The FGH-PCF structure assures important optical communication qualities such birefringence (B), ultra-high negative optical dispersion rate ($D(\lambda)$, high nonlinear coefficient ($\gamma$), confinement loss ($L_c$), and large effective optical area ($A_{\text{eff}}$), which determine the mode of communication across the fiber. This structure is more robust and promising than previous designs. The suggested structure was simulated using the full commercial vector element modeling tool COMSOL Multiphysics version 4.2. The refractive index (RI) of the flint glass material utilized in the proposed structure may be calculated using Sellmeier's equation (Brückner, 2014).

$$n^2(\lambda) = 1 + \frac{B_1\lambda^2}{\lambda^2 - C_1} + \frac{B_2\lambda^2}{\lambda^2 - C_2} + \frac{B_3\lambda^2}{\lambda^2 - C_3} \tag{1}$$

In this context, the RI of flint glass is designated as "n" and is calculated using Sellmeier constants: $B_1 = 1.34533359$, $B_2 = 0.209073176$, $B_3 = 0.937357162$, $C_1 = 0.00997743871$ μm$^2$, $C_2 = 0.0470450767$ μm$^2$, and $C_3 = 111.886764$ μm$^2$. These constants are particular to the flint glass material (lead (II) oxide doped silica) at $T = 20°C$.

However, Maxwell's effective vector RI ($n_{\text{eff}}$) is employed to determine the most acceptable modal value of the RI. Equation (2), as described in O'Shea (2004), provides the computation method for $n_{eff}$.

$$n_{eff} = \frac{\beta(\lambda, n_m(\lambda))}{k_0} \tag{2}$$

The wave's propagation constant is indicated as β and $k_0$ denotes the wave number in free space, where is the wavelength. The modal effective index ($n_{eff}$) is calculated by utilizing the FEM to solve an eigenvalue issue. The optical dispersion rate has a considerable impact on the efficiency of optical wave transmission. After determining $n_{eff}$, essential parameters like chromatic dispersion ($D(\lambda)$, confinement loss ($L_c$), and birefringence ($B$) may be estimated using specialized formulae. These obtained properties are critical in evaluating the performance and features of the optical system, providing significant insights into its behavior and prospective applications.

$$D(\lambda) = -\left(\frac{\lambda}{c}\right)\left(\frac{d^2 Re[n_{eff}]}{d\lambda^2}\right) \quad ps/(nm \bullet km) \tag{3}$$

$$L_c = 8.686 \times k_0 Im[n_{eff}] \quad dB/m \tag{4}$$

$$B = |n_x - n_y| \tag{5}$$

The effective area, $A_{eff}$, is determined as follows from Equation (6) (Mortensen, 2002):

$$A_{eff} = \frac{(\iint |\vec{E}|^2 dxdy)^2}{\iint |\vec{E}|^4 dxdy} \quad \mu m^2 \tag{6}$$

Understanding the nonlinear processes that occur in PCFs requires a thorough understanding of the effective area, $A_{eff}$, which is measured in square micrometers (μm$^2$) and is dependent on the amplitude of the electric field $\vec{E}$, inside the medium.

The ratio between the Kerr constant (nonlinear RI coefficient), $n_2 = 21.2 \times 10^{-20}$ m$^2$/W for dense flint glass commercially known as Schott SF-6 glass (Weber et al., 1978), and the effective mode area at a specific wavelength of the optical field is an important criterion for determining the strength of nonlinear effects. The nonlinear coefficient is proportional to the effective mode area and is computed as follows:

$$\gamma = \frac{2\pi n_2}{\lambda A_{eff}} \quad W^{-1}km^{-1} \tag{7}$$

## 4. Numerical Outcome Analysis

Across various wavelengths, the effective RI of flint glass may be computed using both Sellmeier's equation and the FEM. We discover various effective refractive indices when we examine each fundamental mode between 1280 and 1790 nm. Figure 2 depicts the wavelength versus effective RI plot for both $x$ and $y$ polarization modes. Within this wavelength range, the RI ranges from 1.475 to 1.39 for both polarization modes.

**Figure 2**
**Plot of wavelength versus effective refractive index for $x$ and $y$ polarization**

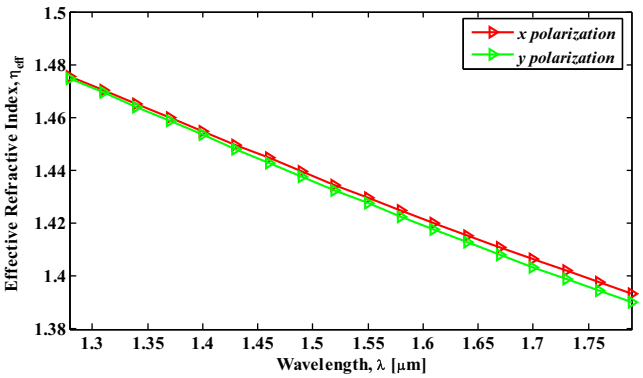


In Figure 3, wavelength dependent chromatic dispersion curve is shown. The flint glass has Abbe number lower than 50 that make it a dispersive material and can cause dispersion in communication bands. The proposed honeycomb combination with the optimum design

**Figure 3**
**Chromatic dispersion graph for $x$ and $y$ polarization based on wavelength**

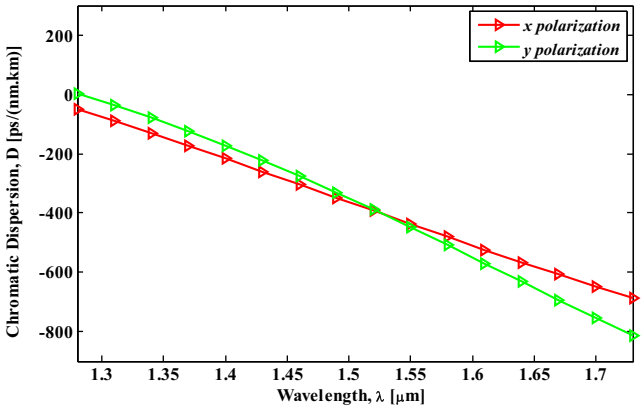

value successfully compensates the dispersion values in telecommunication wavelength band. The curve shows the dispersion compensating property of the proposed FGH-PCF fiber in the E to L wavelength range. The result shows the negative dispersion values of − 436.6 ps/(nm.km) for x polarization and − 448.1 ps/(nm.km) for y polarization at 1550 nm operating wavelength.

The fiber's resilience in terms of dispersion compensation properties was evaluated by altering the pitch value to ±1% for both *x* and *y* polarization modes. The observations for ±1% variation of pitch value are shown in Figure 4. For x polarization mode with pitch varying to ±1% leads dispersion coefficient value to -421.3 and -451.9 ps/(nm.km), respectively, at a wavelength of 1550 nm. Similar evaluations were done for the y polarization mode and the dispersion value ranges between -432.4 and -463.7 ps/(nm.km), respectively, for ±1% variation in the pitch value. It was discovered that increasing the pitch value resulted in an increase in dispersion, but decreasing the pitch value resulted in a considerable drop in dispersion.

The FGH-PCF's birefringence properties are seen in Figure 5. It was discovered that the findings are on the order of $10^{-3}$ after observing the birefringence throughout the wavelength range of 1280–1790 nm. In comparison to contemporary developments and study findings, this amount of birefringence is not generally regarded as being extremely high. It was discovered that the FGH-PCF had a birefringence of $2.202\times10^{-3}$ at a wavelength of 1550 nm.

In Figure 6, the variation in birefringence for ±1% change in optimum pitch value is presented. These observations demonstrate the sensitivity of the birefringence in response to changes in the pitch value of the FGH-PCF. The optimal pitch value of 0.9 **µ**m appears to yield the most desirable birefringence outcome, while deviating from this value in either direction leads to significant changes in the birefringence characteristics of the fiber. For 1% increase in pitch value decreases the birefringence value to $2.147 \times 10^{-3}$ and 1% decrease in pitch value demonstrates increment in birefringence to $2.258 \times 10^{-3}$ at 1550 nm wavelength. These findings are essential for fine-tuning the FGH-PCF's performance in applications where precise birefringence control is crucial.

The astounding nonlinear characteristics of the FGH-PCF's x and y polarization modes are displayed in Figure 7. The fiber had a very high nonlinear coefficient at the working wavelength of 1550 nm, measuring 558.8 $W^{-1}$ $km^{-1}$ for x polarization and 547.9 $W^{-1}$ $km^{-1}$ for y polarization. In contrast to previously used silica material, the flint glass material exhibited substantially higher nonlinearity. This difference in nonlinearity can be attributed to the higher Kerr constant possessed by flint glass compared to silica. The elevated Kerr constant in flint glass is a key factor contributing to its exceptional nonlinear characteristics.

These findings highlight the potential advantages of utilizing flint glass material in the FGH-PCF, as it offers superior nonlinear properties compared to traditional silica-based fibers. Such enhanced nonlinear behavior opens up new possibilities for the fiber's application in various nonlinear optics and photonics technologies.

Figure 8 displays the wavelength-dependent effective area calculations. At a wavelength of 1550 nm, the effective area for x polarization is measured to be 1.538 **µ**m², while for y polarization, it is 1.569 **µ**m².

Confinement loss, also known as propagation loss, plays a crucial role in the design of PCFs. Figure 9 illustrates the FGH-PCF's wavelength dependency of the confinement loss, revealing remarkably low losses of 2.289 dB/cm for x polarization and 4.935 dB/cm for y polarization at 1550 nm. These low confinement losses at 1550 nm demonstrate the effectiveness of

**Figure 4**
**Chromatic dispersion for *x* and *y* polarization exhibits wavelength-dependent behavior, which varies with ±1% of pitch values**

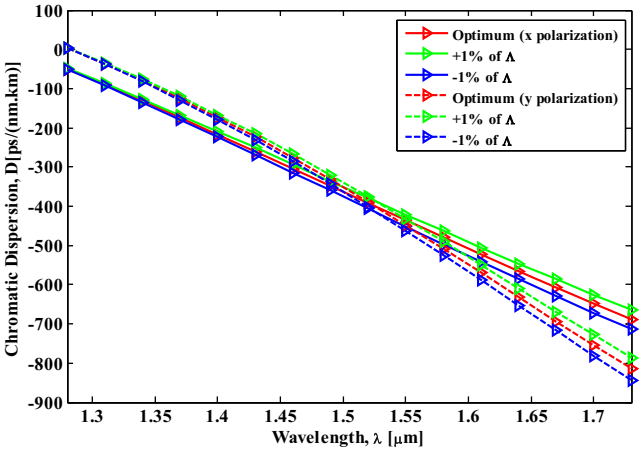


**Figure 5**
**Optimal wavelength versus birefringence plot of proposed FGH-PCF**

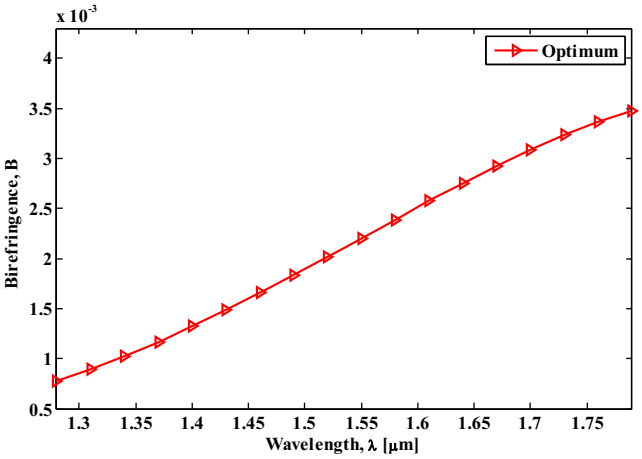


**Figure 6**
**Wavelength versus birefringence plot of proposed FGH-PCF for ±1% variation in pitch values**

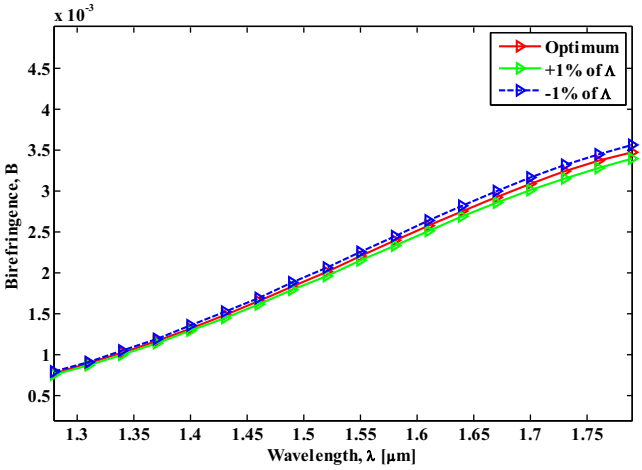

**Figure 7**
**Comparison of wavelength versus nonlinear coefficient for *x* and *y* polarization**

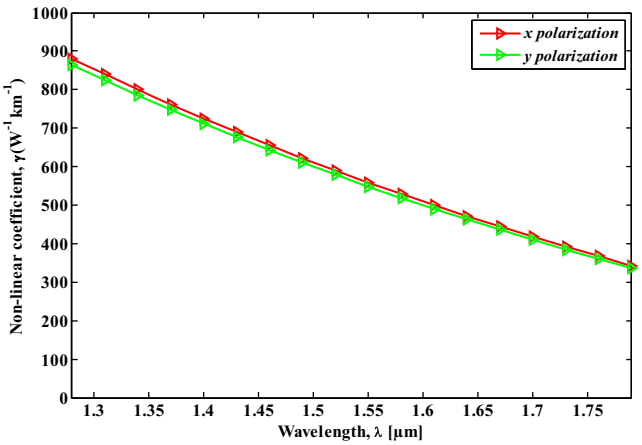


**Figure 8**
**Plot illustrating the relationship between wavelength and effective area for *x* and *y* polarization**

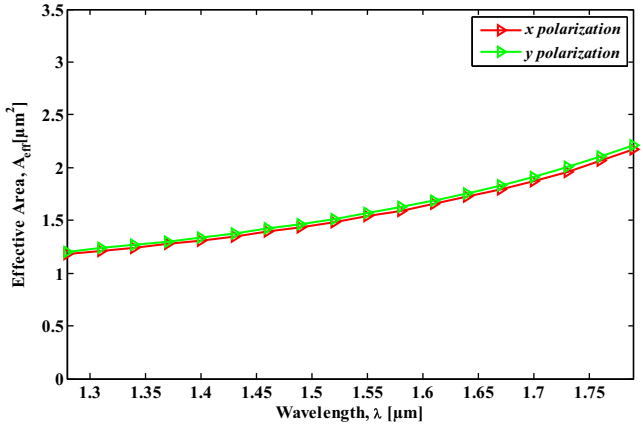


the PCF design in maintaining efficient light confinement within the fiber. Such low losses are highly desirable for various optical communication and sensing applications, as they ensure minimal signal degradation and improved overall performance (Ali & Farhood, 2019).

**Figure 9**
**Confinement loss of the suggested FGH-PCF curve obtained for *x* and *y* polarization with the optimum design parameters**

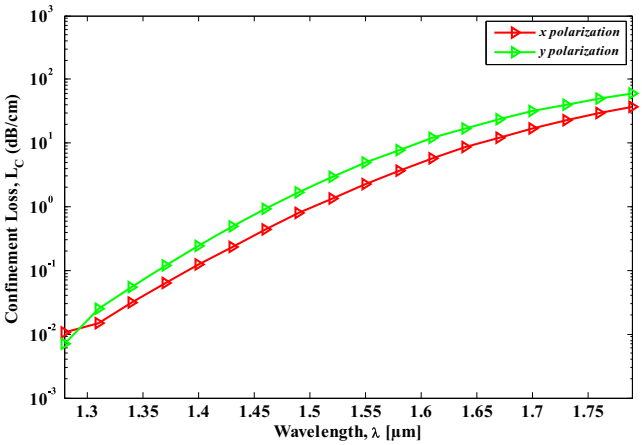


**Figure 10**
**At the optical wavelength of = 1.55 μm, the electric field distributions of several basic modes for the FGH-PCF are shown in (a) *x* polarization and (b) with an arrow pointing in the direction of the electric field**

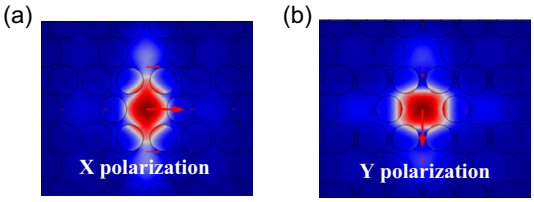


The suggested FGH-PCF's *X*- and *Y*-polarization mode distributions at 1550 nm operating wavelength are shown in Figure 10.

A comparison of the planned FGH-PCF with earlier PCFs is shown in Table 1. The outcomes unequivocally show that the suggested FGH-PCF performs better than the findings of recently published studies.

**Table 1**
**Assessment of required optical properties between the proposed PCF and previously reported PCFs is provided at the operating wavelength of $\lambda = 1550$ nm**

| Ref. | Cladding material | Nonlinear coefficient, $\gamma$ [$W^{-1}$ $km^{-1}$] | Effective area, $A_{eff}$ [$\mu m^2$] | Dispersion, D [ps/(nm.km)] |
|---|---|---|---|---|
| Hasan et al. (2016) | Silica-xenon filling | $6.74\times10^{-3}$ | – | – |
| Islam et al. (2017) | Silica | 92.83 | 1.35 | −1694.80 |
| Prajapati et al. (2019) | Silica | 21.23 | 5.36 | −722.48 |
| Halder and Anower (2019) | Silica | 33.76 | 2.762 | –378.6 |
| Halder (2020) | Silica | 50.34 | 2.327 | − 606 |
| Paul et al. (2022) | Silica | 74.68 | 1.77 | −2357.54 |
| Singh et al. (2022) | Silica | 85 | – | −597 |
| Proposed FGH-PCF | Lead (II) oxide-doped silica | 558.8 | 1.538 | −448.1 |

## 5. Conclusion

In conclusion, the highly nonlinear FGH-PCF operating at 1550 nm wavelength demonstrates exceptional properties for diverse nonlinear optical applications. Utilizing the unique honeycomb lattice structure and nonlinear characteristics of flint glass, advanced numerical simulations and optimization techniques tailored the PCF's dispersion and nonlinear effects. Experimental characterization confirmed its high birefringence, low confinement losses, and significant dispersion compensation capabilities −436.6 ps/(nm.km) for x polarization and −448.1 ps/(nm.km) for y polarization. Moreover, the FGH-PCF exhibited a remarkably high nonlinear coefficient, making it promising for four-wave mixing (Robert et al., 2020), supercontinuum generation (Wadsworth et al., 2002), frequency conversion (Bonsma-Fisher et al., 2022), and parametric amplification (Pakarzadeh et al., 2016). Due to its dispersion compensating and highly nonlinear (558.8 $W^{-1}$ $km^{-1}$) nature, the proposed FGH-PCF is more suitable for supercontinuum generation applications for 1550 nm pump wavelength. Its integration into optical communication systems can lead to compact and efficient nonlinear devices, meeting the demands of high-speed and high-capacity networks. Future research in this domain has the potential to delve deeper into refining the design of FGH-PCF. This could involve delving into innovative compositions of flint glass or exploring alternative materials with significantly higher nonlinear coefficients. Addressing integration challenges, such as creating durable connectors, could be a pivotal area of exploration. Moreover, studies could shift toward real-world implementation, evaluating how FGH-PCF performs in practical communication networks. Furthermore, delving into applications in cutting-edge fields like quantum communication or integrated photonics could unlock new realms for research and development.

## Funding Support

The authors declare that there was no external funding for the research reported in this article.

## Ethical Statement

This study does not contain any studies with human or animal subjects performed by any of the authors.

## Conflicts of Interest

The authors declare that they have no conflicts of interest to this work.

## Data Availability Statement

Data sharing is not applicable to this article as no new data were created or analyzed in this study.

## References

Ali, A. H., & Farhood, A. D. (2019). Design and performance analysis of the WDM schemes for radio over fiber system with different fiber propagation losses. *Fibers*, *7*(3), 19. https://doi.org/10.3390/fib7030019

Bjarklev, A., Broeng, J., & Bjarklev, A. S. (2003). *Photonic crystal fibres*. USA: Springer.

Bonsma-Fisher, K. A. G., Bustard, P. J., Parry, C., Wright, T. A., England, D. G., Sussman, B. J., & Mosley, P. J. (2022). Ultratunable quantum frequency conversion in photonic crystal fiber. *Physical Review Letters*, *129*(20), 203603. https://doi.org/10.1103/PhysRevLett.129.203603

Brain, C. (2002). The technology of 17th century flint glass. In *Proceedings of the XIX International Congress on Glass*, *43*, 357–360.

Broeng, J., Mogilevstev, D., Barkou, S. E., & Bjarklev, A. (1999). Photonic crystal fibers: A new class of optical waveguides. *Optical Fiber Technology*, *5*(3), 305–330. https://doi.org/10.1006/ofte.1998.0279

Brückner, V. (2014). *To the use of Sellmeier formula*. Retrieved from: https://www.researchgate.net/publication/262294649_To_the_use_of_Sellmeier_formula

Cavillon, M., Kucera, C., Hawkins, T., Dawson, J., Dragic, P. D., & Ballato, J. (2018). A unified materials approach to mitigating optical nonlinearities in optical fiber. III. Canonical examples and materials road map. *International Journal of Applied Glass Science*, *9*(4), 447–470. https://doi.org/10.1111/ijag.12336

Dudley, J. M., & Taylor, J. R. (2009). Ten years of nonlinear optics in photonic crystal fibre. *Nature Photonics*, *3*(2), 85–90. https://doi.org/10.1038/nphoton.2008.285

El Hamzaoui, H., Bouazaoui, M., & Capoen, B. (2020). Sol–gel materials for optical fibers. In A. Martucci, L. Santos, R. E. R. Hernández & R. Almeida (Eds.), *Sol-gel derived optical and photonic materials* (pp. 315–346). Netherlands: Elsevier. https://doi.org/10.1016/B978-0-12-818019-8.00014-4

Halder, A. (2020). Slope matched highly birefringent hybrid dispersion compensating fiber over telecommunication bands with low confinement loss. *Journal of Optics*, *49*(2), 187–195. https://doi.org/10.1007/s12596-020-00606-6

Halder, A., & Anower, M. S. (2019). Relative dispersion slope matched highly birefringent and highly nonlinear dispersion compensating hybrid photonic crystal fiber. *Photonics and Nanostructures-Fundamentals and Applications*, *35*, 100704. https://doi.org/10.1016/j.photonics.2019.100704

Hasan, M. I., Akhmediev, N., & Chang, W. (2016). Mid-infrared supercontinuum generation in supercritical xenon-filled hollow-core negative curvature fibers. *Optics Letters*, *41*(21), 5122–5125. https://doi.org/10.1364/OL.41.005122

Islam, M. I., Khatun, M., & Ahmed, K. (2017). Ultra-high negative dispersion compensating square lattice based single mode photonic crystal fiber with high nonlinearity. *Optical Review*, *24*(2), 147–155. https://doi.org/10.1007/s10043-017-0308-0

Jagota, V., Sethi, A. P. S., & Kumar, K. (2013). Finite element method: An overview. *Walailak Journal of Science and Technology*, *10*(1), 1–8.

Karamifard, M. (2022). Assessment of photonic crystal fibers for dispersion factor of different structure. *Journal of Applied Dynamic Systems and Control*, *5*(1), 21–25.

Mortensen, N. A. (2002). Effective area of photonic crystal fibers. *Optics Express*, *10*(7), 341–348. https://doi.org/10.1364/OE.10.000341

O'Shea, D. C. (2004). *Diffractive optics: Design, fabrication, and test*. USA: SPIE Press.

Pakarzadeh, H., Taghizadeh, M., & Hatami, M. (2016). Designing a photonic crystal fiber for an ultra-broadband parametric amplification in telecommunication region. *Journal of Nonlinear Optical Physics & Materials*, *25*(2), 1650023. https://doi.org/10.1142/S0218863516500235

Papadopoulos, M. G., Sadlej, A. J., & Leszczynski, J. (2006). *Non-linear optical properties of matter: From molecules to condensed phases*. Netherlands: Springer.

Paul, B. K., Ahmed, K., Rani, M. T., Pradeep, K. S., & Al-Zahrani, F. A. (2022). Ultra-high negative dispersion compensating

modified square shape photonic crystal fiber for optical broadband communication. *Alexandria Engineering Journal*, *61*(4), 2799–2806. https://doi.org/10.1016/j.aej.2021.08.006

Prajapati, Y. K., Kumar, R., & Singh, V. (2019). Design of a photonic crystal fiber for dispersion compensation and sensing applications using modified air holes of the cladding. *Brazilian Journal of Physics*, *49*(5), 745–751. https://doi.org/10.1007/s13538-019-00686-1

Pysz, D., Kujawa, I., Stępień, R., Klimczak, M., Filipkowski, A., Franczyk, M., . . . , & Buczyński, R. (2014). Stack and draw fabrication of soft glass microstructured fiber optics. *Bulletin of the Polish Academy of Sciences: Technical Sciences*, *62*(4), 667–682. https://doi.org/10.2478/bpasts-2014-0073

Robert, P., Fourcade-Dutin, C., Dauliat, R., Jamier, R., Muñoz-Marco, H., Pérez-Millán, P., . . . , & Bigourd, D. (2020). Spectral correlation of four-wave mixing generated in a photonic crystal fiber pumped by a chirped pulse. *Optics Letters*, *45*(15), 4148–4151. https://doi.org/10.1364/OL.398614

Schodek, D. L., Ferreira, P., & Ashby, M. F. (2009). *Nanomaterials, nanotechnologies and design: An introduction for engineers and architects*. Netherlands: Elsevier.

Singh, S., Upadhyay, A., Sharma, D., & Taya, S. A. (2022). A comprehensive study of large negative dispersion and highly nonlinear perforated core PCF: Theoretical insight. *Physica Scripta*, *97*(6), 065504. https://doi.org/10.1088/1402-4896/ac6d1a

Wadsworth, W. J., Ortigosa-Blanch, A., Knight, J. C., Birks, T. A., Man, T. P. M., & Russell, P. S. J. (2002). Supercontinuum generation in photonic crystal fibers and optical fiber tapers: A novel light source. *Journal of the Optical Society of America B*, *19*(9), 2148–2155. https://doi.org/10.1364/JOSAB.19.002148

Wang, S., Li, Z., Yu, C., Wang, M., Feng, S., Zhou, Q., . . . , & Hu, L. (2013). Fabrication and laser behaviors of $Yb^{3+}$ doped silica large mode area photonic crystal fiber prepared by sol–gel method. *Optical Materials*, *35*(9), 1752–1755. https://doi.org/10.1016/j.optmat.2013.05.029

Webb, K. E., Erkintalo, M., Xu, Y., Broderick, N. G., Dudley, J. M., Genty, G., & Murdoch, S. G. (2014). Nonlinear optics of fibre event horizons. *Nature Communications*, *5*(1), 4969. https://doi.org/10.1038/ncomms5969

Weber, M. J., Milam, D., & Smith, W. L. (1978). Nonlinear refractive index of glasses and crystals. *Optical Engineering*, *17*(5), 175463. https://doi.org/10.1117/12.7972266

Weiner, A. M. (2011). *Ultrafast optics*. USA: Wiley.

Zhang, P., Zhang, J., Yang, P., Dai, S., Wang, X., & Zhang, W. (2015). Fabrication of chalcogenide glass photonic crystal fibers with mechanical drilling. *Optical Fiber Technology*, *26*, 176–179. https://doi.org/10.1016/j.yofte.2015.09.002

Zhou, G., Hou, Z., Li, S., & Hou, L. (2006). Fabrication of glass photonic crystal fibers with a die-cast process. *Applied Optics*, *45*(18), 4433–4436. https://doi.org/10.1364/AO.45.004433

**How to Cite:** Halder, A., Tanshen, M. R., Hossain, M. A., Akter, M. S., & Sikdar, M. A. (2024). Tailored Dispersion and Nonlinear Effects in Flint Glass Honeycomb PCF for Optical Communication. *Journal of Optics and Photonics Research*. *1*(1), 43–49. https://doi.org/10.47852/bonviewJOPR32021750